Revista Brasileira de Cartografia (2017), Edição de Fotogrametia e Sensoriamento Remoto, Nº 69/6: 1117-1125
Sociedade Brasileira de Cartografia, Geodésia, Fotogrametria e Sensoriamento Remoto
ISSN: 1808-0936

ATMOSPHERIC CORRECTIONS OF OLI LANDSAT IMAGES WITH HORIZONTAL VISIBILITY DATA FROM FIELD OBSERVATIONS AND AIRPORT

Correções Atmosféricas de Imagens OLI Landsat 8 com Dados de Visibilidade Horizontal de Campo e de Aeroporto

Isadora Ferreira Bolpato[1], Mauro Antonio Homem Antunes[1], Yuri Andrei Gelsleichter[2], Lúcia Helena Cunha dos Anjos[2] & Paula Debiasi[1]

[1]Federal Rural University of Rio de Janeiro - UFRRJ
Inst. de Tecnologia/Dep. de Engenharia
Seropédica – RJ, Brazil – CEP: 23897-000
isadora.bolpato@hotmail.com, homemantunes@gmail.com, pauladebiasi@yahoo.com.br

[2]Federal Rural University of Rio de Janeiro - UFRRJ
Inst. de Agronomia/Dep. de Solos
Seropédica – RJ, Brazil – CEP: 23897-000
{yuriplanta, lanjosrural}@gmail.com, pauladebiasi@yahoo.com.br

Received on November 19, 2017/ Accepted on December 12, 2017
Recebido em 19 de Novembro, 2017/ Aceito em 12 de Dezembro, 2017

ABSTRACT

The accurate use of satellite images for mapping and environmental monitoring requires the image transformation to ground reflectance through atmospheric correction. However, it is a challenge to obtain the horizontal visibility, which is used by the atmospheric correction models to estimate the aerosol optical depth. The aim of this paper is to present the comparison of atmospheric correction of OLI Landsat 8 images using horizontal visibility from field observation and from airport data. OLI images were acquired from four dates, 02/26/2014, 02/10/2014, 10/11/2015 and 04/20/2016. Field work was conducted at the same time of satellite overpass and horizontal visibility was obtained by observing targets at different distances and recording the maximum distance at which targets could be identifiable by visual inspection yielding values from 12 to 17 km. For comparison the horizontal visibility was also downloaded from METAR database for the Galeão airport, which were up to 10km. Atmospheric correction was carried out for the two sources of horizontal visibility using the *Atmcor4OLI* program, adapted through the 6S code. These two methods were compared through graphs and a statistical test from samples of four targets using apparent and surface reflectance. The results show that the atmospheric correction is paramount to analyze the spectral response of targets as the atmosphere interferes with the spectral characteristics of the targets from the visible to the mid infrared. In the visible the additive effects predominate while in the near and mid infrared the subtractive effects dominate. The visibility of the airport and from field observation yielded surface reflectance values which were different by the test of means at 1% and not significant at the 5%, as the field observations were not much higher than 10 km. It is concluded that an accurate source of horizontal visibility is key for obtaining correct surface reflectance values, mainly when field observation at the time of satellite overpass was not possible.

Keywords: Surface Reflectance, Atmospheric Optical Depth, Image Radiometric Correction.

RESUMO

A correta utilização de imagens de satélite para o mapeamento e monitoramento ambiental requer a transformação destas em medidas físicas, sendo o ideal transformar para reflectância da superfície. No entanto, um desafio é a obtenção da visibilidade horizontal, a partir da qual os modelos obtêm a profundidade óptica de aerossóis. Este artigo tem por objetivo apresentar a correção atmosférica de imagens OLI do Landsat 8 utilizando a visibilidade horizontal estimada por observações de campo e de dados de aeroporto. As imagens OLI Landsat 8 utilizadas foram das datas 26/02/2014, 10/02/2014, 11/10/2015 e 20/04/2016. No instante de passagem do satélite foram realizados trabalhos de campo em que alvos a distâncias conhecidas foram observados para a estimativa da visibilidade horizontal. Para estas datas foram obtidos os dados METAR de visibilidade horizontal do aeroporto do Galeão. As imagens foram corrigidas dos efeitos atmosféricos através do programa *Atmcor4OLI* desenvolvido a partir do código 6S e importadas no software de processamento de imagens para a avaliação dos resultados. Os valores de visibilidade horizontal por meio dos dados do aeroporto Galeão se limitaram a10km enquanto que para as observações de campo a visibilidade variou de 12 a 17 km. A reflectância da superfície de quatro alvos (água limpa, água com sedimentos, solo exposto e floresta) foi utilizada para comparar com os valores de reflectância aparente. A comparação entre os dois métodos de obtenção da visibilidade horizontal foi feita por meio de gráficos e de teste estatístico. Os resultados mostraram que a correção atmosférica é fundamental para se analisar a resposta espectral dos alvos, uma vez que a resposta espectral fica descaracterizada pela atmosfera do visível até o infravermelho médio. No visível predominaram os efeitos aditivos e no infravermelho próximo e médio o efeito subtrativo. As diferenças entre as correções atmosféricas com dados de campo e de aeroporto foram significativas por meio do teste de médias a 1% e não significativas a 95%, uma vez que as observações de campo foram pouco acima de 10 km. Para aplicar a correção atmosférica, deve-se atentar para a obtenção de dados de visibilidade que representem bem a realidade da atmosfera no momento de passagem do satélite, principalmente para os casos em que não foi possível realizar observações de profundidade óptica de aerossóis em campo.

Palavras-chave: Reflectância da Superfície, Profundidade Óptica de Aerossóis, Correção Radiométrica de Imagens.

1. INTRODUCTION

Atmospheric correction is applied to remotely sensed images to eliminate the effects from the atmosphere, reducing the influence of gases and aerosols. The atmosphere is a source of error as it alters the radiance reaching the sensor, leading to image degradation. Thus atmospheric correction is of paramount importance for environmental studies based on spectral properties of features of interest. Even spectral indices of targets will differ greatly if no atmospheric correction is applied (MYNENI & ASRAR, 1994).

The use of the images without the appropriate radiometric corrections can lead to misinterpretation, particularly when comparing different sensors, different dates and involves the use of vegetation indices (ANTUNES, *et al.*, 2012). Thus, it is necessary to perform atmospheric corrections on the images to lessen the atmospheric effects. The procedure involves not only the application of sensor calibration to obtain the radiance at satellite level but also the transformation of this in the satellite level reflectance and then in surface reflectance. This last transformation requires the use of a radiative transfer model for the quantification of the atmospheric effects in the images. Moran *et al.* (1992) found that the use of the radiative transfer model is more advisable for atmospheric corrections than using the dark pixel subtraction method proposed by Chavez (1988).

The atmospheric correction is sensitive to horizontal visibility and therefore care must be taken to use an appropriate methodology to obtain these values (ANTUNES & DEBIASI, 2015, MAIA *et al.*, 2015). Horizontal visibility, classified as the maximum distance at which an observer can see and identify an object that is close to the horizontal plane, is determined by the mass and size distribution of aerosols in the air, which may originate from natural or through human activities. From the horizontal visibility the model calculates the aerosol optical depth, which is used in radiative transfer to compute the Mie scattering and absorption by aerosols.

The ability to perform the horizontal visibility estimates involves some factors such as distance from observer, the visual acuity of the observer, the target position in relation to the observer and the presence of obstructing elements between the observer and

the target. The identification of ground targets by distance is restricted by the scattering of electromagnetic radiation by the atmosphere, thus giving the possibility to obtain the density of suspended aerosols from the horizontal visibility. For satellite image atmospheric corrections, horizontal visibility should ideally be obtained from field observations at the same time of satellite overpass in the area of interest. However, for images already collected for which there were no field observation of visibility, it is possible to obtain these values from airports close to the area of interest or from aerosol optical depth data from MOD04 product of MODIS sensor (REMER *et al.*, 2005). However, this last option has problems due to large failure on the data, being unavailable for the vast majority of situations.

The Landsat 8 satellite was launched on February 11, 2013 (ROY *et al.*, 2014) with two sensors on board, the Operational Land Imager (OLI) which collects images in the solar spectrum and the Thermal Infrared Sensor (TIR) collects images in the thermal infrared. These sensors are part of the series Landsat data continuity and have great importance in monitoring and mapping the Earth's surface. In this work we used the OLI sensor and Table 1 shows its characteristics.

OLI surface reflectance of water has been evaluated using aerosol corrections from the Aerosol Robotic Network Ocean Color (AERONET-OC) sites (PAHLEVAN *et al.*, 2017). However, for most situations there is pronounced difficulty in estimating the horizontal visibility data to perform atmospheric corrections, mainly of images of databases for which there is no possibility of conducting field observations (SANTOS *et al.*, 2017). Thus, this study is aimed at evaluating the results of atmospheric corrections in OLI Landsat 8 images for horizontal visibility from observations in the field and from airports close to the study area.

2. MATERIAL AND METHODS

Orthorectified OLI Landsat 8 images (L1T) from orbit/row 217/76 collected on February 10, 2014, February 26, 2014, October 11, 2015 and April 20, 2016 were used in this work. Terrain correction of OLI images uses cubic convolution resampling. Although this slightly alters original pixel values, the L1T was used in this research to represent the situation of atmospheric corrections by users. In fact, the L1T is the standard USGS processing for OLI images and has been used in other evaluations of atmospheric aerosol correction (e.g., PAHLEVAN *et al.*, 2014, PAHLEVAN *et al.*, 2017).

The horizontal visibility values were acquired in two ways. First were obtained through the observation of horizontal visibility to targets located at known distances from a fixed point. The observation consisted on verifying whether the targets like vegetation cover and rocks at different distances were visible and identifiable, being the horizontal visibility the average distance between the farthest target visible and identifiable and the next target (in distance) which was not identifiable from the observation point. The field works were conducted on the same dates and time of the Landsat 8 satellite. The observed targets were looked from the coordinates 22°46'51"S and 43°40'58"W, located on the campus of the Federal Rural University of Rio de Janeiro (UFRRJ) and the targets were mountains located in the surroundings, with distances ranging from 7 to 25 km.

Table 1: Characteristics of OLI sensor

Spectral resolution from Full Width at Half Maxi-mum (FWHM)	Band 1 – Blue: 0.43-0.45 µm Band 2 – Blue: 0.45-0.51 µm Band 3 – Green: 0.53-0.59 µm Band 4 – Red: 0.64-0.67 µm Band 5 – Near infrared: 0.85-0.88 µm Band 6 – Mid infrared: 1.57-1.65 µm Band 7 – Mid infrared: 2.11-2.29 µm Band 8 – panchromatic: 0.50-0.68 µm Band 9 – Cirrus: 1.36-1.38 µm
Radio-metric resolution	12 bits
Temporal resolution	16 days
Spatial resolution	30 m (15 m for pan)

Source: Roy *et al.* (2014).

The other source of visibility data consisted of download METAR (Meteorological Aerodrome Report) from Galeão airport, located in the city of Rio de Janeiro. These visibility data are given in kilometers with the limit of 10 km. For the condition of no clouds the visibility of 9999 or "CAVOK" (Ceiling And Visibility OK) means that the horizontal visibility is above 10 km. These data were downloaded from the REDEMET network (https://www.redemet.aer.mil.br).

The OLI sensor images were imported to the SPRING software (CÂMARA *et al.*, 1996) and bands one to seven were exported in raw format to perform atmospheric corrections with the Atmcor4OLI model (ANTUNES and DEBIASI, 2015). These corrections were carried out using the visibility from field observations and visibility obtained from the airport data. Visibility values obtained in the field at the same time of Landsat 8 overpass were 12, 13, 16 and 17 while the METAR data from Galeão airport were 10 km for all dates, since values above 10 km are not registered by most airports where these data are collected. Bands one to seven were also converted to apparent reflectance in the SPRING software for comparison purposes. Surface and apparent reflectance of samples from representative features (water, exposed soil and vegetation) were taken to analyze the results through graphs and the paired t-test. For each target and processing two pixels of uniform areas were sampled for OLI bands 1 to 7.

The Atmcor4OLI model was adapted from code 6S (VERMOTE *et al.*, 1997) for atmospheric corrections of OLI Landsat 8 images in the 16-bit and resulting image stores as surface reflectance in real of 32 bits. The parameters used in the atmospheric corrections are shown in Table 2.

Table 2: Input parameters used in the Atmcor4OLIi model

Processing level: L1T (Terrain corrected)			
OLI Landsat 8 image date			
02/10/2014	02/26/2014	10/11/2015	04/20/2016
UTC decimal hour of the scene center			
12.881748	12.878208	12.866853	12.859030
Sun-Earth distance in Astronomical Units (AU)			
0.9901	0.9868	0.9983	1.0048
Solar elevation			
54.898º	56.961º	59.376º	44.256º
Visibility from field observation			
13 km	16 km	12 km	17 km
Visibility from METAR			
10 km	10 km	10 km	10 km
Gaseous atmospheric model: Tropical			
Aerosols model: Continental			
Longitude of the study area center: -43.682792			
Latitude of the study area center: -22.780867			
Average altitude of the study area: 50 m			

3. RESULTS AND DISCUSSION

The samples from resulting images of surface reflectance from both methods of horizontal visibility were arranged in graphs and compared using the paired t-test for all targets studied in this paper.

3.1 Surface reflectance versus apparent reflectance

First were compared the surface and apparent reflectances to evaluate the effect of atmospheric corrections using the model with field observed visibility values (figures 1 to 3). Figure 1 shows that the water reflectance is quite sensitive to atmospheric correction for both clean water and for water with sediments, mainly in the visible. Pahlevan et al. (2017) found that the OLI surface reflectance of ocean water in the blue channels was overestimated by about 10% in average, as compared to the sensors Visible Infrared Imaging Radiometer Suite (VIIRS) and the Moderate Resolution Imaging Spectroradiometer on board the Aqua platform (MODISA). Thus the results found here for the blue bands might also be overestimated by the same amount. In Figure 2 it is shown that for vegetation the effects of atmospheric correction are different between visible and infrared. For soil (Figure 3) the largest differences occur in the blue bands (1 and 2) and in the mid infrared (bands 6 and 7).

The differences between apparent and surface reflectance shown in figures 1 to 3 emphasize the need for atmospheric corrections when using satellite images. The largest differences were found in the visible bands, in which the scattering is mainly due to gases in the atmosphere (Rayleigh scattering). In the near and mid infrared the differences are smaller and apparent was lower than surface reflectance due to absorption of radiation mostly by water vapor in the atmosphere. The red band is somewhat in a transition where the most dominant effect (either scattering or absorption) will depend on the surface reflectance and on the amount of aerosols. For low surface reflectance in band 4, like vegetation for example (Figure 2), the atmospheric correction reduced the values, thus showing that scattering was more pronounced than the absorption. On the other hand, for the relatively high reflectance of soil (Figure 3), the atmospheric correction increased reflectance values, meaning that the absorption was more important in this case. The consequence of this effect is that atmospheric correction enhances the vegetation indices differences between soil and vegetation, mainly for soils with high reflectance values. Additionally, this raises a question on the applicability of vegetation indices without atmospheric correction.

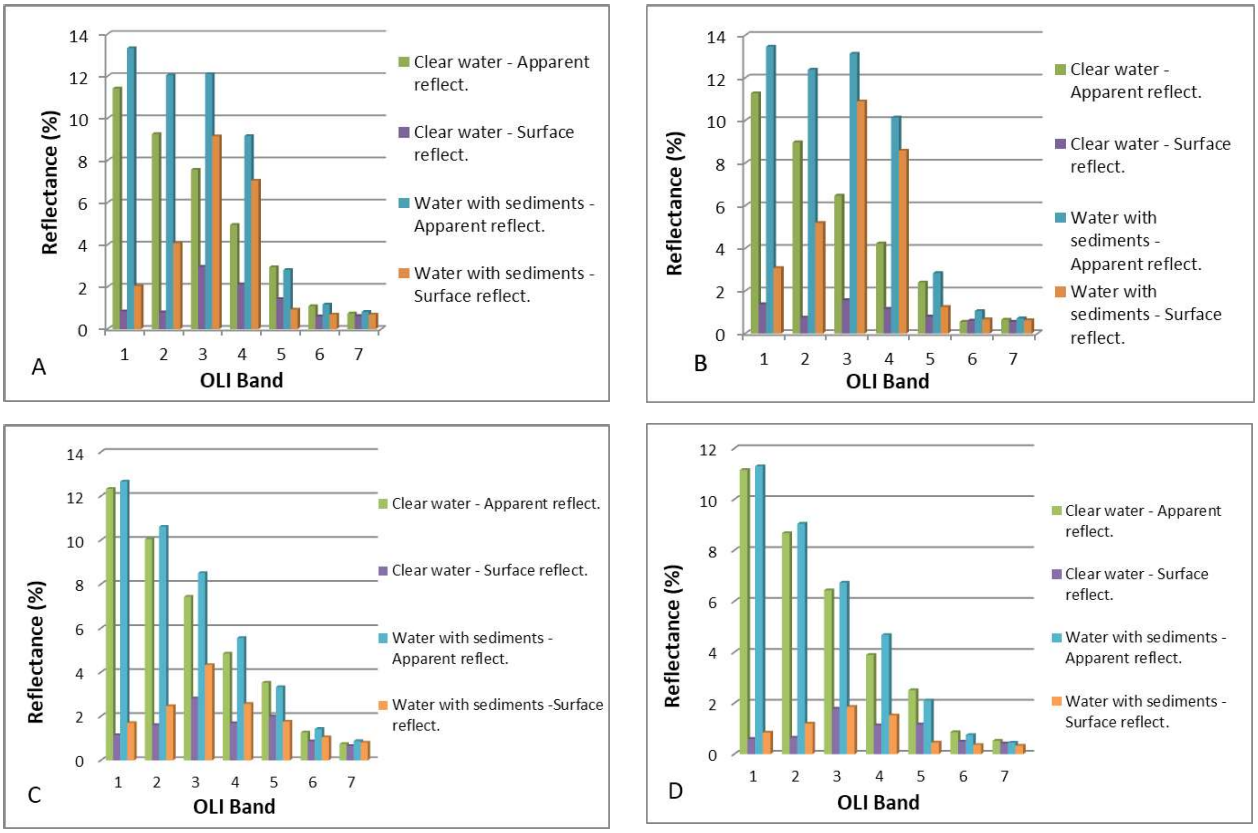

Fig. 1 – Apparent and surface reflectance of clear water and with sediments for each image date. A) 02/10/2014; B) 02/26/2014; C) 10/11/2015; D) 04/20/2016. Visibility values were obtained from field observations.

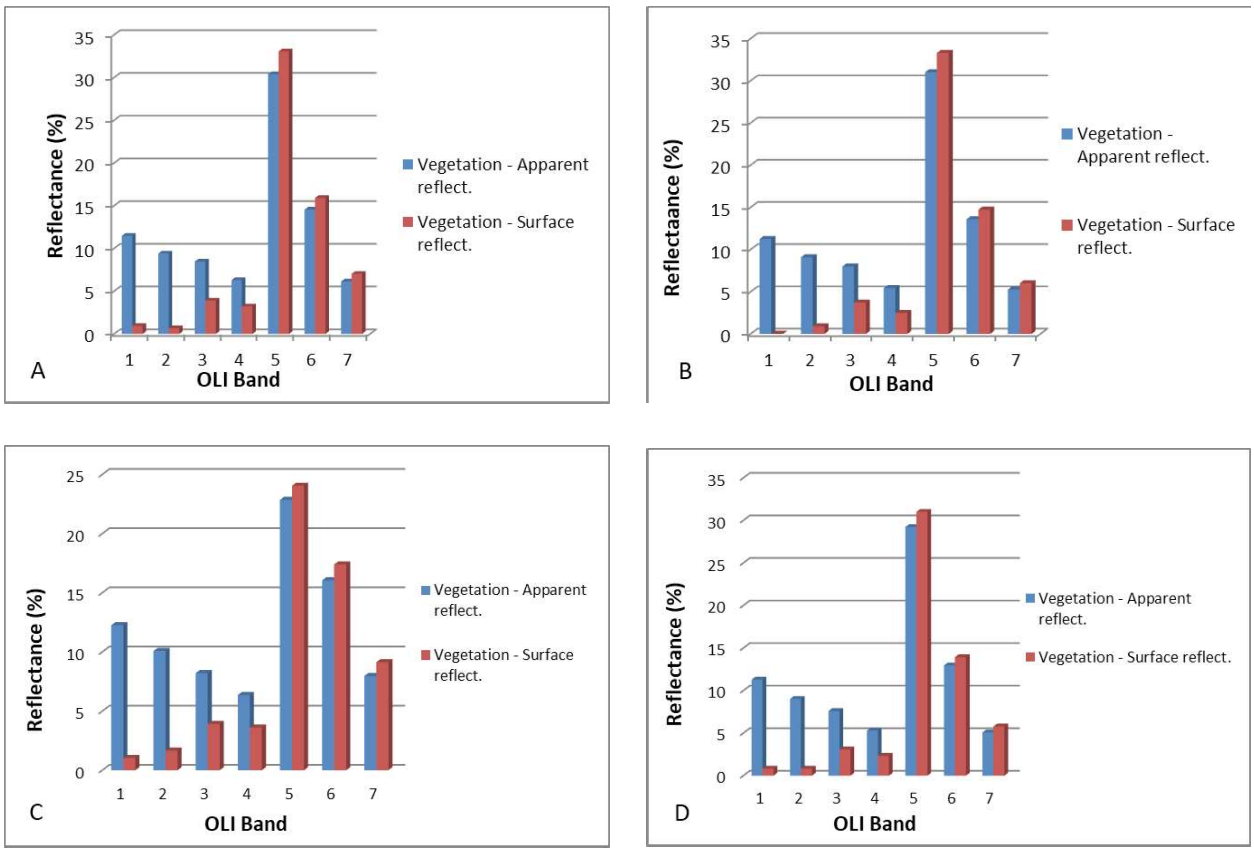

Fig. 2 - Apparent and surface reflectance of forest for each image date. A) 02/10/2014; B) 02/26/2014; C) 10/11/2015; D) 04/20/2016. Visibility values were obtained from field observations.

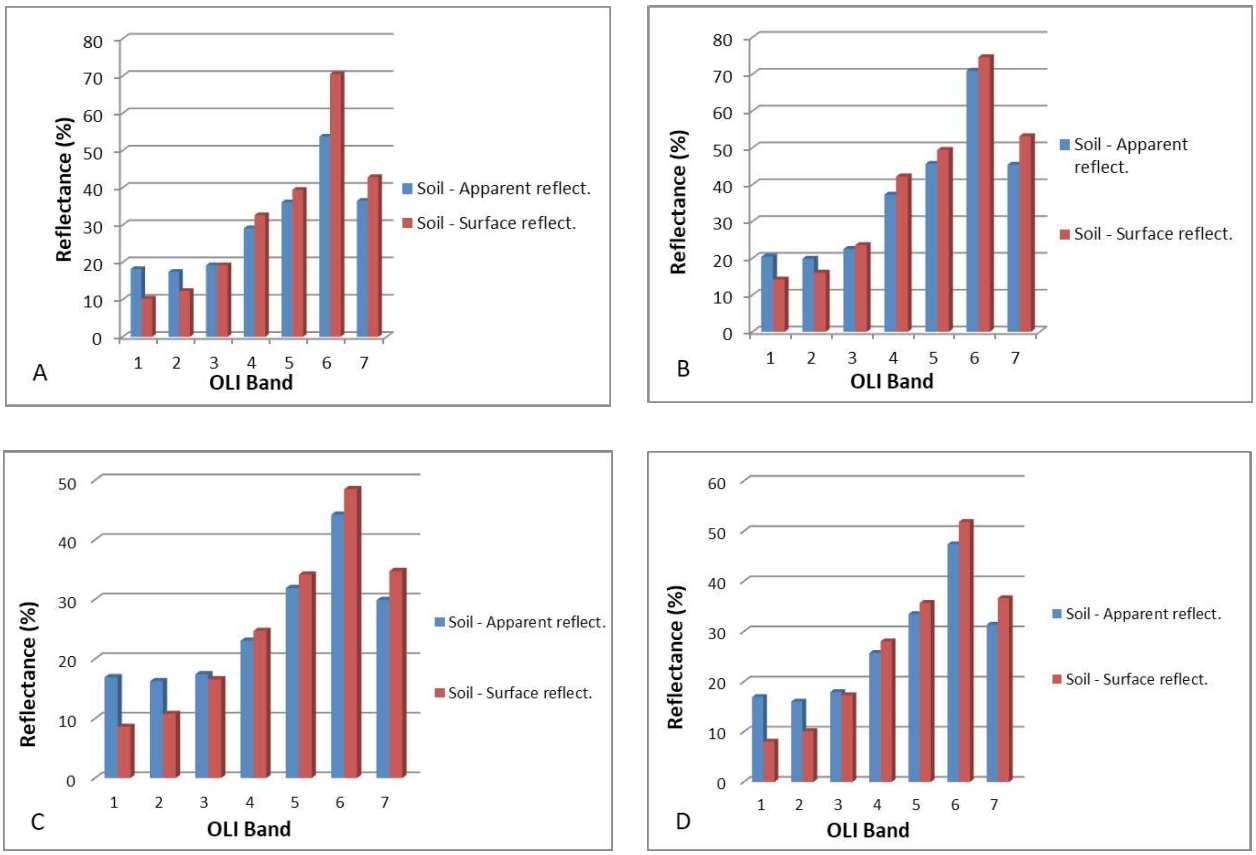

Fig. 3 - Apparent and surface reflectance of bare soil for each image date. A) 02/10/2014; B) 02/26/2014; C) 10/11/2015; D) 04/20/2016. Visibility values were obtained from field observations.

3.2 Comparison of horizontal visibility sources

Graphs of surface reflectance for 10/11/2015 and 04/20/2016 (figures 4 and 5) were generated to compare the sources of horizontal visibility. The field observation yielded respectively 12 km and 17 km of horizontal visibility while the airport data from METAR database had values of 10 km for both dates.

The largest relative differences of surface reflectance between the two sources of horizontal visibility are in the visible part of the spectrum, where the surface reflectance is low for water and vegetation.

The differentiation of horizontal visibility values for the field observation and airport data was larger for 04/20/2016 (17 km and 10 km respectively) than in the image for 10/11/2015 (12 km and 10 km respectively). Then the impact of changing the source of horizontal visibility was higher for the image from 04/20/2016, mainly in the visible bands. For water the differences are higher in the visible bands, where the surface reflectance values are higher than in the infrared bands, mainly for the image from 04/20/2016.

Graphs A and B from Figure 5 show that the use of airport visibility limited to km increased the contribution from Rayleigh scattering, as can be seen in the much higher surface reflectance in the blue bands (1 and 2) calculated using airport visibility. For high values of surface reflectance like in the case of bare soil (bands 3 to 7) and in forest (bands 5 and 6 7) the relative effect of these sources of horizontal visibility are low.

A paired t-test was carried out for the resulting surface reflectance to statistically compare the differences between the two methods of obtaining the horizontal visibility (Table 3). The null hypothesis is that the surface reflectance values are equal to both methods.

By paired t-test the two methods gave results no significant difference at a level of 5%, while for the 99% confidence interval the differences are significant. However, the graphs from figures 4 and 5 show that for the visible bands the differences seem to be expressive. This raises some concerns when studying targets where surface reflectance in the visible part of the spectrum is important. In such cases the source of visibility may play an important role in the obtained results.

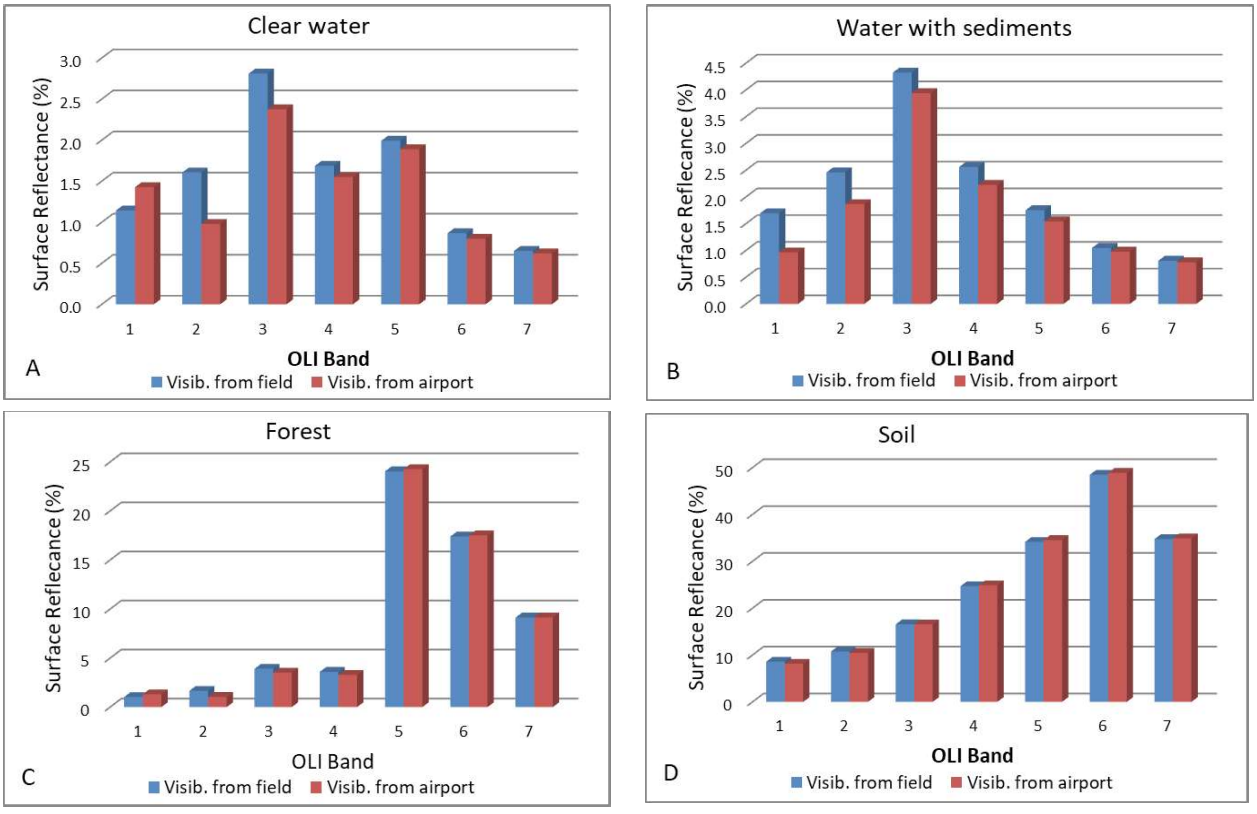

Fig. 4 – Surface reflectance obtained with visibility from field and airport of targets analyzed in this work. Image from 10/11/2015. Horizontal visibility of 12 km for field observation and 10 km for airport.

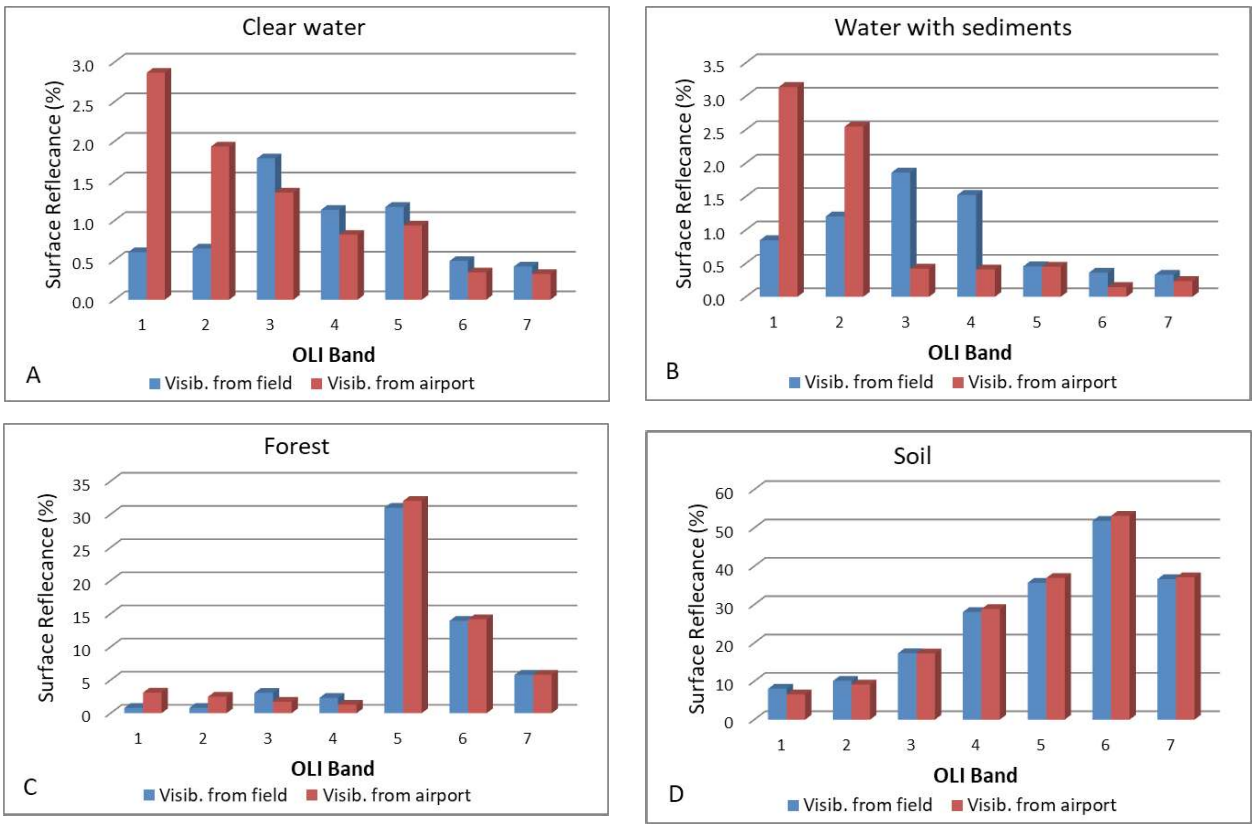

Fig. 5 - Surface reflectance obtained with visibility from field and airport of targets analyzed in this work. Image from 04/20/2016. Horizontal visibility of 17 km for field observation and 10 km for airport.

Table 3: Results of paired t-test for reflectance from horizontal visibility data from field observation and airport

	Field (μ1)	Airport (μ2)
Mean	0.100597978	0.099573001
Variance	0.022064751	0.022008824
Number of observations	112	112
Statistical t	0.561138764	
P(T<=t) two-tailed	0.575834019	p-value for two-tailed
Critical T two-tailed	1.981566757	

4. CONCLUSIONS

The results show that the atmospheric correction is needed for the analysis of remotely sensed images, since the surface reflectance was quite different from the apparent reflectance for all targets analyzed in this study. Additional attention should be taken when using visible and infrared bands in spectral transforms such as vegetation indices. The paired t-test showed that the results of the data differ when using 99% probability. The low differences of the values of surface reflectance by two methods of obtaining horizontal visibility may be attributed to the low differences of horizontal visibility observed the field in relation to the obtained from the airport, which is limited to 10 km. However, graphs show that in the visible bands the differences tend to be higher when the differences between airport and field observation increase. This leads to a caveat for those who use remotely sensed data to study water bodies or other targets with low reflectance in the visible, to use correct values of visibility or aerosol optical depth for correct calculation of surface reflectance. Besides, the visibility achieved through field work generates results closer to what is expected for the target's surface reflectance. Thus, caution should be taken when

using horizontal visibility data from airports, mainly for atmospheric corrections of satellite images when the atmosphere is relatively clean of aerosols (visibility much higher than 10 km). Besides, the validity of airport visibility is geographically limited to the surroundings of the airport. The extent of this validity will depend on weather conditions as well as land use in the area under consideration, as aerosol distribution varies over the surface.

ACKNOWLEDGEMENTS

I. F. Bolpato thanks CNPq for a scholarship grant and Y. A. Gelsleichter thanks CAPES for a scholarship grant.

REFERENCES

ANTUNES, M. A. H., DEBIASI, P. OLI image atmospheric correction sensitivity to altitude, visibility and acquisition geometry. In: 2015 IEEE International Geoscience and Remote Sensing Symposium-IGARSS 2015, Milan, 2015. **Anais**. p. 2245-2248, 2015.

ANTUNES, M. A. H., DEBIASI, P., COSTA, A. R., GLERIANI, J. M. Correção atmosférica de imagens ALOS/AVNIR-2 utilizando o modelo 6S. **Revista Brasileira de Cartografia**, v. 64, n. 4, 531-539, 2012.

CÂMARA, G., SOUZA, R. C. M., FREITAS, U. M., GARRIDO, J. SPRING: Integrating remote sensing and GIS by object-oriented data modeling. **Computers & Graphics**, v. 20, 395-403, 1996.

CHAVEZ, P. S. An improved dark-object subtraction technique for atmospheric scattering correction of multispectral data. **Remote Sensing of Environment**, v. 24, 59-479, 1988.

MAIA, L. H., COUTINHO, L. S., SOUZA, G. M., ANTUNES, M. A. H. Obtenção da reflectância da superfície para imagens OLI do Landsat 8 com um modelo de transferência radiativa. In: XVII Simpósio Brasileiro de Sensoriamento Remoto - SBSR, João Pessoa, 2015. **Anais**. p. 2992-2996, 2015.

MORAN, M. S., JACKSON, R. D., SLATER, P. N., TEILLET, P. M. Evaluation of Simplified Procedures for Retrieval of Land Surface Reflectance Factors from Satellite Sensor Output. **Remote Sensing of Environment**, v. 41, 169-184, 1992.

MYNENI, R. B., ASRAR, G., Atmospheric effects and spectral vegetation indices. **Remote Sensing of Environment**, v. 47, 390-402, 1994.

PAHLEVAN, N., LEE, Z., WEI, J., SCHAAF, C. B., SCHOTT, J. R., BERK, A. On-orbit radiometric characterization of OLI (Landsat-8) for applications in aquatic remote sensing. **Remote Sensing of Environment**, v. 154, 272-284, 2014.

PAHLEVAN, N., SCHOTT, J. R., FRANZ, B. A., ZIBORDI, G. MARKHAM, B., BAILEY, S., SCHAAF, C. B., ONDRUSEK, M., GREB, S., STRAIT, C. M. Landsat 8 remote sensing reflectance (Rrs) products: Evaluations, intercomparisons, and enhancements. **Remote Sensing of Environment**, v. 190, 289-301, 2017.

REMER, L. A., KAUFMAN, Y. J., TANRÉ, D., MATTOO, S., CHU, D. A., MARTINS, J. V., HOLBEN, B. N. The MODIS Aerosol Algorithm, Products, and Validation. **Journal of the Atmospheric Sciences**, v. 62, 947-973, 2005.

ROY, D. P., WULDER, M. A., LOVELAND, T. R., WOODCOCK, C. E., ALLEN, R. G., ANDERSON, M. C., HELDER, D., IRONS, J. R., JOHNSON, D. M., KENNEDY, R., SCAMBOS, T. A., SCHAAF, C. B., SCHOTT, J. R., SHENG, Y., VERMOTE, E. F., BELWARD, A. S., BINDSCHADLER, R., COHEN, W. B., GAO, F., HIPPLE, J. D., HOSTERT, P., HUNTINGTON, J., JUSTICE, C. O., KILIC, A., KOVALSKYY, V., LEE, Z. P., LYMBURNER, L., MASEK, J. G., MCCORKEL, J., SHUAI, Y., TREZZA, R., VOGELMANN, J., WYNNE, R. H., ZHU, Z. Landsat-8: Science and product vision for terrestrial global change research. **Remote Sensing of Environment**, v. 145, 154-172, 2014.

SANTOS, T. C. C., ANTUNES, M. A. H., SEOANE, J. C. S., SOUSA, G. M. Comparação de modelos de correção atmosférica para imagem WorldView-2. **Revista Brasileira de Cartografia**, v. 69, n. 2, 229-240, 2017.

VERMOTE, E. F., TANRÉ, D., DEUZE, J. L., HERMAN, M., MORCETTE, J. J. Second Simulation of the Satellite Signal in the Solar Spectrum, 6S: An overview. **IEEE Transactions on Geoscience and Remote Sensing**, v. 35, 675-686, 1997.